Comparison of the simulated and LIDAR measured atmospheric density and temperature in lower thermosphere

Tian Wan, Guoqing Hu, Jianzheng Jiang, Hongli Liu, Jing Fan, Weilin Pan, and Shuai Qiao

Articles you may be interested in

Comparison of balloon-carried atmospheric motion sensors with Doppler lidar turbulence measurements
Rev. Sci. Instrum. **80**, 026108 (2009); 10.1063/1.3086432

Rocket-borne instrument for measuring vibrational-rotational temperature and density in the lower thermosphere
Rev. Sci. Instrum. **76**, 083101 (2005); 10.1063/1.1988189

A lidar system for measuring atmospheric pressure and temperature profiles
Rev. Sci. Instrum. **58**, 2226 (1987); 10.1063/1.1139327

Molecular Beam Techniques Applied to Mass Spectrometric Thermospheric Density Measurements
Rev. Sci. Instrum. **44**, 1524 (1973); 10.1063/1.1685990

Thermospheric Temperature Measurement Technique
J. Vac. Sci. Technol. **9**, 467 (1972); 10.1116/1.1316658

Comparison of the Simulated and LIDAR Measured Atmospheric Density and Temperature in Lower Thermosphere

Tian Wan[a], Guoqing Hu[a], Jianzheng Jiang[a], Hongli Liu[a], Jing Fan[a]

Weilin Pan[b], Shuai Qiao[b]

[a]State Key Laboratory of High Temperature Gasdynamics, Institute of Mechanics, Chinese Academy of Sciences, Beijing 100190, China
[b]Institute of Atmospheric Physics, Chinese Academy of Sciences, Beijing, 100029, China

Abstract. The atmospheric density and temperature in lower thermosphere are analyzed using numerical simulation, empirical model, satellite data and ground LIDAR measurement. The WACCM global atmosphere model is used as the numerical simulation method; the empirical models include NRLMSISE-00 and US-76; the satellite data are taken by US SABER/TIMED satellite. The atmospheric density and temperature with an altitude range from 60km to 100km at Germu in August 2013 are measured by a ground LIDAR system. Comparison of the results from different methods shows that the density and temperature are in good agreement below altitudes 90km and 80km, respectively. Above the altitudes, the discrepancy between the different methods increases with increasing altitude. It is also noted that the daily and diurnal variation of density and temperature become significant above 100km altitude.

Keywords: lower thermosphere density and temperature, ground LIDAR measurement, global climate simulation
PACS: 92.60.hv, 93.85.Pq, 93.85.Bc

INTRODUCTION

In recent years, the flight corridor of newly appeared near-space vehicles has reached the lower thermosphere. In order to precisely predict the aerodynamic force on the near-space vehicles, further study of the lower thermosphere is required. Traditional research methods include empirical model [1-3], numerical model [4-16], satellite data [17-23], ground radar observation [24-30], and rocket and balloon [31-33]. However, due to lack of observation data at the lower thermosphere, which is typically beyond reach of both ground-based and satellite radar, study on this atmospheric regime is quite limited. As a result, physical modeling of this layer is difficult. Figure 1 is an example of the uncertainty of the density at 100km altitude by using different methods, which shows up to 35% discrepancy based on US-76 standards.

In this paper, a global climate simulation model, Whole Atmosphere Community Climate Model (WACCM) [16] is used to compute atmospheric density and temperature around 100km altitude, and the computed results are compared with LIDAR (Light Detection and Ranging) measurement at Germu in August, 2013. Also compared are the TIMED/SABER (The Sounding of the Atmosphere using Broadband Emission Radiometry), NRLMSISE-00 (Naval Research Laboratory Mass Spectrometer and Incoherent Scatter-00) and US-76 results. In the following sections, the WACCM model is briefly described, followed by introduction of LIDAR measurement. Then the comparison of density and temperature above Germu in August 2013 by using different models are shown.
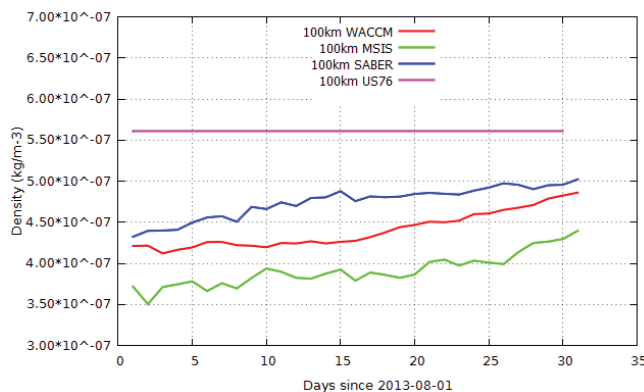

FIGURE 1. Daily density variation predicted by different methods at 100km altitude above Germu in August 2013.

WACCM MODEL

WACCM model is a three-dimensional global climate model developed by National Center of Atmospheric Research in recent years. The latest version, WACCM4, is based on CAM-5.3 (Community Atmosphere Model) atmosphere model, which includes mesosphere/lower thermosphere phenomena, chemistry reactions, dynamic core etc. Numerical methods include finite volume method that is used in this work, spectral element method, etc. From ground to the model top (around 140km), the simulation zone is divided into 66 vertical layers. The vertical resolution is 1.1km in troposphere, 1.1~1.4km in lower stratosphere, 1.75km at stratosphere top, and 3.5km above 65km. The horizontal resolution is 4°×5°. The chemistry model being used is the MOZART (Model for OZone And Related chemical Tracers) chemistry model [34]. WACCM4 is based on the NCAR CESM (Community Earth System Model) that is a coupled model including atmosphere, land, ocean and ice modules. CESM version 1.2 is used in this work. The computation starts with standard data F_2000_WACCM on an in-house built Linux cluster using 64 CPU.

LIDAR MEASUREMENT

The Rayleigh laser radar developed by Institute of Atmospheric Physics, Chinese Academy of Sciences was used to measure the density and temperature above Germu (36.25°N，94.54°E) in August 2013. The range of altitude being measured is from 60km to 100km. The wavelength of the radar was 532nm.

From 30km and above, Mie scattering from aerosols is negligible except in some special occasions such as a volcanic eruption. Therefore, by assuming pure molecular scattering in this region, atmosphere temperature can be derived by combining the hydrostatic equation and ideal gas law as

$$T(z) = T(z_0) \frac{\rho(z_0)}{\rho(z)} + \frac{1}{R} \int_z^{z_0} g(r)dr \frac{\rho(r)}{\rho(z)}, \tag{1}$$

where R is the gas constant for dry air, $g(z)$ and $\rho(z)$ are the gravitational acceleration and number density at the altitude of z, respectively. The seeding temperature $T(z_0)$ at a certain altitude can be adopted from model as the initial estimation.

For Rayleigh scattering, the LIDAR equation for a ground-based LIDAR system is written as

$$N(z) = (\eta T_A^2)\left(\frac{P\Delta t}{h\nu}\right)\left(\sigma_R n(z)\Delta z\right)\left(\frac{A_R}{z^2}\right) + N_B, \tag{2}$$

where $N(z)$ is the total photon numbers received by the telescope of area A_R during time interval Δt corresponding to a height interval Δz in range z, N_B is background noise from solar scattering and PMT dark counts, η is system efficiency, $(P\Delta t / h\nu)$ is the transmitted photon numbers within Δt, σ_R is Rayleigh backscatter cross section, and T_A is one-way atmospheric transmittance. Background noise level N_B is calculated by averaging photon counts from those bins corresponding to high altitude, where Rayleigh scattering does not occur.

By selecting a reference density at a reference altitude

$$\rho(z) = \frac{z^2 \rho(z_0) (N(z) - N_B)}{z_0^2 (N(z_0) - N_B)} \tag{3}$$

In our measurement, 50km is chosen as the reference altitude.

Germu Experiment and Discussion

LIDAR measurement was conducted at Germu in August 2013, and the measured density and temperature are compared with those from WACCM, SABER, and NRLMSISE-00. Figure 2 plots the vertical density and temperature distribution, where the results of NRLMSISE-00, WACCM and SABER are monthly average in August 2013, and LIDAR result is on August 29th, 2013. The theoretical upper limit of SABER is 110km, but the available data is a little lower. The density distributions show that the results below 90km altitude are in good agreement, whereas above 90km, the discrepancy between the five methods increases substantially, especially for LIDAR, which indicates increased error of LIDAR above 90km. The temperature distributions show that the results below 80km altitude are in good agreement, whereas above 80km, the discrepancy increases. Note that at 110km altitude, the temperature result of WACCM and SABER are higher than NRLMSISE-00 and US-76 temperature, and the reason might be that 110km is near the upper limit of WACCM and SABER.
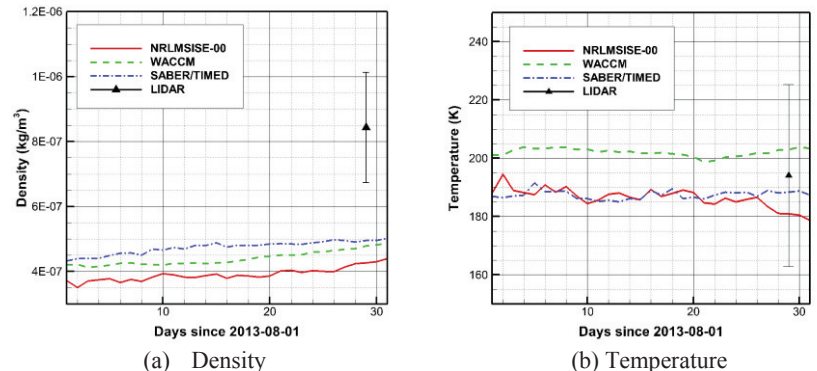
(a) Density   (b) Temperature
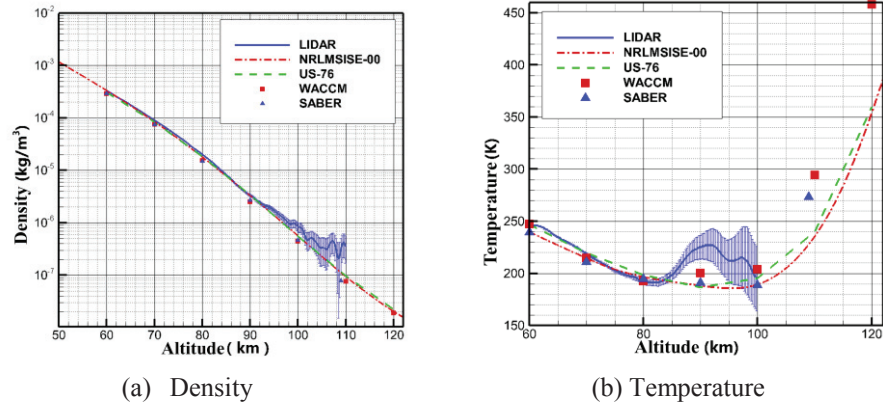
FIGURE 2. Atmospheric density (a) and temperature (b) distribution above Germu in August 2013. The results of NRLMSISE-00, WACCM and SABER are monthly averaged, and LIDAR result is on August 29th, 2013.

Figure 3 is the daily density and temperature variation at 110km altitude, where WACCM and NRLMSISE-00 results are at local time 00:00, and local time of SABER is variable. The density distributions show large error of LIDAR at this altitude. The temperature distributions show same decreasing trend of NRLMSISE-00, WACCM and SABER. Note that the zigzags of SABER temperature are due to variable daily local time of TIMED satellite. Figure 4 is the daily density and temperature variation at 100km altitude. The density distributions of NRLMSISE-00, WACCM and SABER are in similar trend, whereas the error of LIDAR density is still large at this altitude. Similar trend is also observed in the temperature distributions. Figure 5 is the daily density and temperature variation at 90km altitude, which shows smaller discrepancy of density, whereas difference in temperatures of different models is still relatively large.

Among these results, the SABER measured temperature is the most reliable source. At around 110km altitude, NRLMSISE-00 and US76 under-predict temperature, which shows loss of accuracy of these two models at this altitude. 110km is near the top boundary of the WACCM model which may lead to loss of accuracy and the over-predicted temperature at 110km altitude.

(a) Density   (b) Temperature
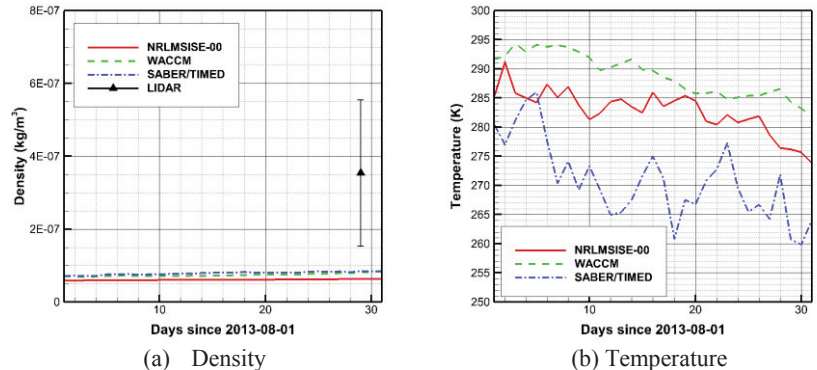
FIGURE 3. Daily variation of density (a) and temperature (b) at 110km above Germu in August 2013.

(a) Density   (b) Temperature

FIGURE 4. Daily variation of density (a) and temperature (b) at 100km above Germu in August 2013.

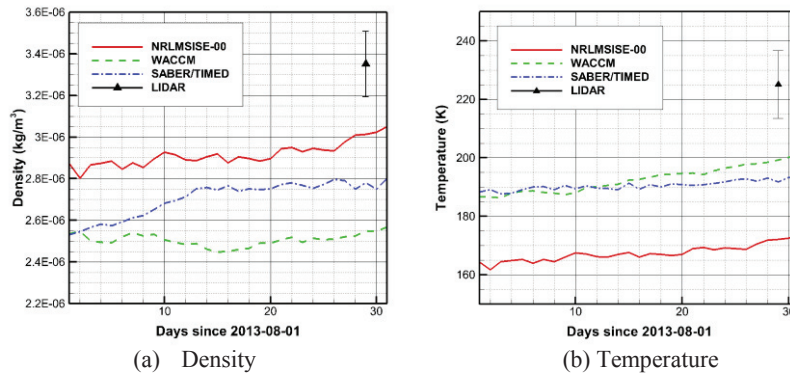|	
(a) Density	(b) Temperature

FIGURE 5. Daily variation of density (a) and temperature (b) at 90km above Germu in August 2013.

CONCLUSIONS

The atmospheric density and temperature in lower thermosphere are not well studied. In this paper, the atmosphere at around 100km altitude above Germu in August 2013 is studied, by using a global climate model WACCM and LIDAR measurement, as well as comparison with empirical models and satellite data. Comparison shows that the densities from the different methods agree for altitudes below 90km, and the temperatures agree for altitudes below 80km. Above these two altitudes, the discrepancy between different methods increases with increasing altitude. Daily variation of density and temperature in August 2013 is plotted, and the trends agree in general, whereas discrepancy increases as altitude increases.

REFERENCES

1.   A Hedin, *Journal of Geophysical Research*, **92**, 4649-4662 (1987).
2.   A Hedin, *Journal of Geophysical Research*, **96**, 1159-1172 (1991).
3.   J M Picone, A E Hedin, D P Drob, A C Aikin, *Journal of Geophysical Research,* **107**, 1-16 (2002).
4.   R E Dickinson, E C Ridley, R G Roble, *Journal of Geophysical Research,* **86**, 1499-1512 (1981).
5.   R E Dickinson, E C Ridley, R G Roble, *Journal of the Atmospheric Sciences,* **41**, 205-219 (1984).
6.   R G Roble, E C Ridley, R E Dickinson, *Journal of Geophysical Research,* **92**, 8745-8758 (1987).
7.   R G Roble, E C Ridley, A D Richmond, R E Dickinson, *Geophysical Research Letters*, **15**, 1325-1328 (1988).
8.   A D Richmond, E C Ridley, R G Roble, *Geophysical Research Letters*, **19**, 601-604 (1992).
9.   R G Roble, E C Ridley, *Geophysical Research Letters*, **21**, 417-420 (1994).
10. W Wang, *Journal of Atmospheric and Solar-Terrestrial Physics*, **61**, 385-397 (1999).
11. T J Fuller-Rowell, D Rees, *Journal of the Atmospheric Sciences,* **37**, 2545-2567 (1980).
12. T J Fuller-Rowell, D Rees, *Planetary and Space Science*, **31**, 1209 (1983).
13. D Rees, T J Fuller-Rowell, *Planetary and Space Science*, **36**, 935 (1988).
14. D Rees, T J Fuller-Rowell, *Advances in Space Research*, **10**, 83-102 (1990).
15. M J Harris, N F Arnold, A D Aylward, *Annals of Geophysics*, **20**, 225-235 (2002).
16. R R Garcia, *Journal of Geophysical Research* **112**, 1-23 (2007).
17. The Solar Mesosphere Explorer, 2014, see http://lasp.colorado.edu/sme.
18. Upper Atmospheric Research Satellite (UARS) Project Scientific Office Page, 2014, see http://umpgal.gsfc.nasa.gov.
19. C A Reber, etc, *Journal of Geophysical Research,* **98**, 10643-10648 (1993).
20. Earthnet Online, European Space Agency, 2014, see http://earth.esa.int/object/index.cfm.
21. TIMED: A mission to explore one of the last frontiers in Earth's atmosphere, 2014, see http://www.timed.jhuapl.edu.
22. ESA missions, Envisat, 2014, see http://envisat.esa.int/.
23. Goddard Space Flight Center, Aura's HQ Homepage, 2014, see http://aura.gsfc.nasa.gov.
24. F Q Li, etc, *Chinese Journal of Space Science*, **22**, 65-71 (2002).
25. J G Xiong, F Yi, *Chinese Journal of Space Science*, **4**, 318-323 (2001).
26. T E Van Zandt, *Annales Geophysicae*, **18**, 740-749 (2000).
27. S Fukao, etc, *Radio Science*, **25**, 477-485 (1990).
28. J H Qiu, etc, *Chinese Journal of Space Science*, **4**, 318-323 (2001).
29. R L Collins, D Thorsen, S J Franke, *Journal of Geophysical Research*, **102**, 16583-16592 (1997).
30. W Pan, S G Chester, G R Raymond, *Geophysical Research Letters*, **29**, 1-4 (2002).

31. T Abe, etc, "Coordinated rocket and ground-based observations of neutral temperature during the dynamics and energetics of the lower thermosphere in Aurora (DELTA) Campaign" in Amer. Geophys. Uni. Fall meeting, 2005.
32. G T Qin, etc, *Chinese Journal of Space Science*, **22**, 136-141 (2002).
33. G T Qin, etc, *Chinese Journal of Space Science*, **23**, 135-141 (2003).
34. L K Emmons, etc, *Geoscientific Model Development*, **3**, 43-67 (2010).